J. Fluid Mech. (2010), *vol.* 661, *pp.* 522–539. © Cambridge University Press 2010
doi:10.1017/S002211201000323X

Suppressing van der Waals driven rupture through shear

M. J. DAVIS, M. B. GRATTON† AND S. H. DAVIS

Department of Engineering Sciences and Applied Mathematics, McCormick School of Engineering and Applied Science, Northwestern University, Evanston, IL 60208, USA

(Received 29 January 2010; revised 9 June 2010; accepted 9 June 2010; first published online 18 August 2010)

An ultra-thin viscous film on a substrate is susceptible to rupture instabilities driven by van der Waals attractions. When a unidirectional 'wind' shear τ is applied to the free surface, the rupture instability in two dimensions is suppressed when τ exceeds a critical value τ_c and is replaced by a permanent finite-amplitude structure, an intermolecular-capillary wave, that travels at approximately the speed of the surface. For small amplitudes, the wave is governed by the Kuramoto–Sivashinsky equation. If three-dimensional disturbances are allowed, the shear is decoupled from disturbances perpendicular to the flow, and line rupture would occur. In this case, replacing the unidirectional shear with a shear whose direction rotates with angular speed, $\hat{\omega}$, suppresses the rupture if $\tau \gtrsim 2\tau_c$. For the most dangerous wavenumber, $\tau_c \approx 10^{-2}\,\mathrm{dyn\,cm^{-2}}$ at $\hat{\omega} \approx 1\,\mathrm{rad\,s^{-1}}$ for a film with physical properties similar to water at a thickness of 100 nm.

Key words: coating, instability, lubrication theory

1. Introduction

Thin liquid films may spontaneously rupture due to van der Waals forces. Such ruptures are inconveniences in many applications, leading to the breakdown of foams or the dewetting of liquid layers into drops. Instabilities are important in applications as diverse as lithographic printing (Lenz & Kumar 2007), tear films (Holly 1973; King-Smith *et al.* 2004) and coating flows (Reiter 1992; Jacobs, Herminghaus & Mecke 1998).

For films on substrates, rupture may occur if the film does not wet the substrate. Experiments by Sheludko (1967) showed that for a uniform liquid film of thickness approximately 100 nm deposited on a non-wettable substrate, the liquid may develop dry spots and eventually break into droplets. Ruckenstein & Jain (1974) developed a model for the van der Waals force between a uniform film and a substrate, and used linear stability theory to show that such films are vulnerable to rupture through long-wave instability. As the instability grows, the nonlinear behaviour leads to holes opening in the film in finite time (Williams & Davis 1982; Zhang & Lister 1999; Witelski & Bernoff 2000). For films with two free surfaces, the same van der Waals instability persists due to the attraction between the two liquid–gas interfaces. Moreover, the van der Waals forces are always attractive between the interfaces leading to rupture in films that are sufficiently thin (Vrij 1966). Again, linear stability

† Email address for correspondence: m-gratton@northwestern.edu

https://doi.org/10.1017/S002211201000323X Published online by Cambridge University Press

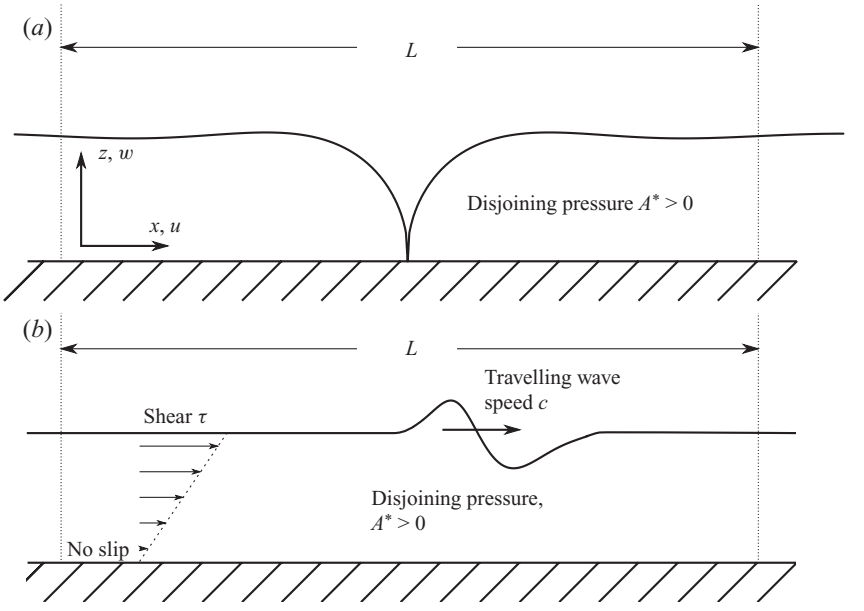


FIGURE 1. A diagram of a two-dimensional film (*a*) without applied shear and (*b*) with applied shear.

theory (Sharma & Ruckenstein 1986; Ida & Miksis 1998) shows that there is a long-wave instability, and nonlinear effects lead to finite-time self-similar rupture (Erneux & Davis 1993; Vaynblat, Lister & Witelski 2001).

Several authors have observed experimentally that flow in a thin film can stabilize the film, as discussed in a review by Coons *et al.* (2003). However, all of these studies are for heavily surfactant-laden interfaces that effectively make the interfaces immobile. These results are consistent with the theory by Gumerman & Homsy (1975), who calculated that for a radial geometry with no-slip conditions at the two interfaces, flow improves the stability of a free film.

Anderson, Brush & Davis (2010) have found that even uncontaminated free films are substantially stabilized by flow. They consider a foam lamella, where flow is caused by the highly curved Plateau borders inducing capillary pressure gradients, leading to a uniform thinning flow with a stagnation point at the centre of the lamella. They calculated that the flow, along with the edge geometry, make the threshold film thickness for rupture as much as 10 times smaller (about 10 nm) than the threshold for rupture of a bounded planar film without flow.

We assess to what degree flow can stabilize a film against rupture in a canonical model that eliminates the complications of surfactants and the degeneracy of the free-film case. The basic domain, shown in figure 1(*a*), is a spatially periodic region of size L. The intermolecular forces between the film surface and the substrate are taken to be attractive, so the Hamaker constant $A^* > 0$ and disturbances will grow, ultimately leading to dewetting of the liquid in finite time. The result from Ruckenstein & Jain (1974) shows that films on domains of size at least

$$L_c = \left(\frac{A^*}{2\pi\sigma h_0^4}\right)^{1/2}, \tag{1.1}$$

https://doi.org/10.1017/S002211201000323X Published online by Cambridge University Press

are unstable, where σ is the surface tension and h_0 is the unperturbed film height. Moreover, the growth rate of disturbances from linear theory is maximized for disturbances with wavelengths

$$L_M = \sqrt{2}L_c. \tag{1.2}$$

We first consider a two-dimensional disturbance $h = h(x, t)$ and choose a periodic domain whose size is at least $L > L_c$; typically, we consider $L = L_M$. We introduce a 'wind' shear of magnitude τ (shown in figure 1*b*) that induces a flow. For a uniform film, this gives a linear velocity profile $u(z) = (\tau/\mu)z$. We find for sufficiently large τ, that rupture is suppressed and replaced by a permanent travelling solution: an intermolecular-capillary wave with wave speed c closely related to the shear strength. We here present a proof of concept: shear can stabilize films at magnitudes that are small enough to be practical.

Work by Bielarz & Kalliadasis (2003) prefigures this study, as they also found that a bounded thin film with an imposed mean flow was stabilized against van der Waals rupture if the flow was large enough. Recently, Kalpathy, Francis & Kumar (2010) discussed a similar problem in which the upper layer of a two liquid-layer system is sheared. The physics for the two-fluid problem differs from the prototype model we discuss here, but they also find that there is a critical shear rate that suppresses rupture.

For small amplitudes, the wave is a solution of the Kuramoto–Sivashinsky (KS) equation. The magnitude of the shear modulates only the amplitude, while longer periodic domains result in complex dynamics and chaos. Similar waves are observed in other film problems with similar hyperbolic terms arising from other physical effects. For falling films with moderate Reynolds numbers, the body force of gravity introduces the hyperbolic term, while the film is destabilized by inertial effects that grow with the film thickness (Chang 1994; Chang *et al.* 1996). For thin films, an inclined substrate can again provide a gravitational body force similar to surface shear. Thiele & Knobloch (2004) examined the dynamics of thin liquid films on inclined and heated substrates and find similar waves to those we see here. Thiele *et al.* (2002) consider drops on an inclined plane. The film equations are regularized with a diffuse interface model that adds a wetting potential with a conjoining component. Tseluiko & Papageorgiou (2006*b*) consider an electrified falling film, where again the hyperbolic term arises from gravity but the film is destabilized now by a non-local term due to the electric field. In the companion paper, they show that the small amplitude equations are non-local KS equations with chaotic dynamics (Tseluiko & Papageorgiou 2006*a*).

Whereas the dynamics for small amplitude disturbances are the same for thin falling films, thin films with a mean flow and thin films with surface shear, the shear magnitude required to suppress rupture is far less than the required body force. In one dimension, the governing equations take the form

$$h_t + m_b(h^3)_x + (h^3 h_{xxx} + h^{-1}h_x)_x = 0, \tag{1.3}$$

for a body force of magnitude m_b and

$$h_t + m_s(h^2)_x + (h^3 h_{xxx} + h^{-1}h_x)_x = 0, \tag{1.4}$$

for a surface shear of magnitude m_s. For the two hyperbolic terms to be comparable, $m_b \approx m_s/h$. Thus, body forces must be $O(h^{-1})$ larger than surface shears to have similar magnitudes. As h is small, this difference in scale is crucial to the practicality of rupture suppression through shear.

https://doi.org/10.1017/S002211201000323X Published online by Cambridge University Press

We also consider the three-dimensional problem, where $h = h(x, y, t)$. Again we use a periodic domain with $0 \leqslant x < L_M$ and $0 \leqslant y < L_M$. If the shear is unidirectional, rupture may be prevented in the direction of shear, but line rupture occurs in the cross-stream direction. In order to suppress rupture in all directions, we borrow an idea from Schulze & Davis (1995) and introduce a constant-magnitude rotating shear with angular frequency $\hat{\omega}$. We show that the complete shear protocol $(\hat{\omega}, \tau)$ can again stabilize the film against rupture and lead to a permanent, three-dimensional travelling wave. We observe that the minimum magnitude of shear needed to stabilize a three-dimensional film is about twice the magnitude needed to stabilize a two-dimensional film for the optimum shear frequency.

2. Lubrication theory

Consider a liquid layer of infinite extent in the xy plane, with a rigid substrate at $z = 0$ and a free surface at $z = h(x, y, t)$. The film (see figure 1) is composed of an incompressible Newtonian liquid with constant viscosity μ, density ρ and surface tension σ. The mean height of the film h_o is small (about 100 nm) compared to typical length scales, so that the aspect ratio $\varepsilon \ll 1$. The film does not wet the substrate, subjecting the film to attractive van der Waals forces with Hamaker constant $A^* > 0$. We model this force with the usual disjoining pressure

$$U'(h) = \tfrac{1}{3}h^{-3}. \tag{2.1}$$

In principle, here the analysis could be extended to cover more general wetting potentials $U(h)$ representing other surface forces, including those modelling partial wetting (Teletzke, Davis & Scriven 1988; Vignes-Adler 2002). The wetting potential would be augmented to be $U(h) = -(h^{-2}/6) + Bh^{-m}$ for $m > 2$ and a positive constant B. This added term is only important for very small values of h. In addition, the term is stabilizing; it acts against the van der Waals of potential. If rupture is suppressed with (2.1), then h will never become small enough for conjoining forces to matter, and so they will be omitted. A constant shear stress of magnitude τ and unit direction $\boldsymbol{e}$ is applied tangent to the surface, entering the problem through the tangential stress balance. Such a shear could be generated by uniform air flow away from the surface and would naturally move tangent to h near the surface of liquid. Following standard lubrication theory (Oron, Davis & Bankoff 1997), film height, lateral distance and time are non-dimensionalized by

$$z' = h_o z, \quad h' = h_o h, \quad (x', y') = \frac{h_o}{\varepsilon}(x, y), \quad t' = \frac{h_o}{U_c}t, \tag{2.2}$$

where primed quantities are dimensional, h_o is the height scale, ε is the small aspect ratio and $U_c = \sigma/\mu$ is the capillary velocity scale. We note that the condition that the shear is tangent to the surface is, at leading order, equivalent to it being parallel to the xy plane, as $h'_{x'} = O(\varepsilon)$. Expanding in ε gives the non-dimensional equation

$$h_t + \theta \boldsymbol{e} \cdot (h \nabla h) + \nabla \cdot (S h^3 \nabla \nabla^2 h + A h^{-1} \nabla h) = 0, \tag{2.3}$$

at leading order, where $\nabla = (\partial/\partial x, \partial/\partial y)$ is the two-dimensional gradient and subscripts denote differentiation. The parameters in (2.3) are

$$\theta = \frac{\tau h_o}{\sigma}, \quad S = \frac{\varepsilon^3}{3} \quad \text{and} \quad A = \frac{\varepsilon A^*}{6\pi\sigma h_o^2}. \tag{2.4}$$

https://doi.org/10.1017/S002211201000323X Published online by Cambridge University Press

A is the Sheludko number, measuring the relative magnitude of van der Waals forces to surface tension. S is the rescaled inverse capillary number, where because of the choice of velocity scale σ and μ do not appear. The scale here arises from insisting that surface tension appear in the governing equations at leading order (Oron *et al.* 1997). The magnitude of the shear is controlled by θ.

Equation (2.3) may be rescaled to eliminate A and S in favour of a single parameter describing the shear by defining

$$x = X, \quad y = Y, \quad h = \left(\frac{A}{S}\right)^{1/4} H, \quad t = S^{-1/4}A^{-3/4}T. \tag{2.5}$$

We avoid scaling the lateral lengths so that the range of linearly unstable wavenumbers does not change as the shear is varied. Inserting these scales results in the evolution equation

$$H_T + \beta \boldsymbol{e}\cdot(H\nabla H) + \nabla\cdot(H^3\nabla\nabla^2 H + H^{-1}\nabla H) = 0, \tag{2.6}$$

with shear parameter

$$\beta = \frac{\theta}{\sqrt{SA}} = \sqrt{\frac{18\pi}{\sigma A^*}}\left(\frac{h_o}{\varepsilon}\right)^2 \tau. \tag{2.7}$$

The effective shear strength scales on the length scale h_o/ε, and is inversely proportional to the surface forces.

We first look to determine the stability of infinitesimal perturbations through normal-mode analysis. We define a base state as a uniform film of height H_0 and introduce plane-wave perturbations

$$\hat{H} = H_0 + \delta \mathrm{e}^{qT + \mathrm{i}\boldsymbol{k}\cdot\boldsymbol{X}}, \tag{2.8}$$

and linearize in amplitude $\delta \ll 1$. This gives the dispersion relation for $k = |\boldsymbol{k}|$,

$$q = H_0^3 k^2(H_0^{-4} - k^2) - \mathrm{i}H_0\boldsymbol{k}\cdot(\beta\boldsymbol{e}), \tag{2.9}$$

which is the same as for the unsheared problem (Ruckenstein & Jain 1974; Williams & Davis 1982) except for an imaginary term corresponding to travelling waves. From this, we can determine that the basic state $H = H_0$ has a long-wave instability that is unaffected by the magnitude of the shear. Features such as the most dangerous wavenumber

$$k_M = 2^{-1/2}H_0^{-2}, \tag{2.10}$$

corresponding to the maximum growth rate, and the cutoff wavenumber $k_c = H_0^{-2}$, corresponding to neutral stability, do not depend on β. However, this analysis only tells us whether infinitesimal perturbations will grow, but not whether rupture will occur, as rupture requires finite-sized amplitude changes in H.

In order to determine the effect of shear on rupture, we must consider the full nonlinear equation. The equation has two parameters, β and

$$H_0 = \left(\frac{2\pi\varepsilon^2\sigma}{A^*}\right)^{1/4} h_o^{1/2}. \tag{2.11}$$

For fixed liquid properties, H_0 will vary with the film thickness as $h_o^{1/2}$. While β also depends on h_o, the shear may be independently adjusted to get any value for β. We mainly consider the case of $H_0 = 1$, corresponding to $h_o = 10^{-5}$ cm for material properties similar to those of water (see § 6). This case represents a typical dewetting

https://doi.org/10.1017/S002211201000323X Published online by Cambridge University Press

film. In the discussion, we will examine how the critical shear rate to suppress rupture varies in order of magnitude with the film thickness h_o.

3. Numerical solutions

Numerical solutions to (2.6) in two and three dimensions with periodic boundary conditions are computed using two techniques: a pseudo-spectral fourth-order explicit time-stepping method and a second-order in time and space implicit scheme. The explicit scheme can achieve spectral accuracy, allowing for the use of fairly coarse grids. We found 64 points to be sufficient in two dimensions and 32×32 acceptable in three dimensions, provided rupture does not occur. Close to rupture, the film steepens and more modes are needed to resolve the dynamics. However, as we are looking to suppress rupture, very accurate descriptions of the near-rupture dynamics are not necessary. When rupture does not occur, this scheme is quite successful at mapping the behaviour of the system.

Closer to rupture, we use an implicit scheme with second-order centred differences in space and a Crank–Nicholson scheme in time. We find that the extra temporal accuracy is necessary to resolve the dynamics when an external shear is applied. With only first-order time-stepping, travelling-wave solutions decay in amplitude. In two dimensions, the periodic boundary conditions are handled by using the Woodbury formula. In three dimensions, the larger stencil and extra boundaries magnify the difficulty from the periodic boundary condition. For convenience, we use the PARDISO Krylov solver for sparse systems (Schenk, Waecher & Hagermann 2007; Schenk, Bollhoefer & Roemer 2008), an iterative matrix solver that operates on matrices in sparse-row format.

4. Suppression of rupture in two dimensions

We first consider the effect of shear on rupture in the XZ-plane, appropriate to systems that are narrow in the Y-direction ($L_2 < L_c$), neglecting the effects of a curved meniscus. The evolution equation (2.6) for $H(X, T)$ is reduced to

$$H_T + \beta H H_X + (H^3 H_{XXX} + H^{-1} H_X)_X = 0. \tag{4.1}$$

We enforce periodic boundary conditions on an interval $[0, L_M]$, with $L_M = 2\sqrt{2}\pi$.

4.1. *Numerical results*

We compute the full solution of (4.1) numerically using the two methods described in § 3. Figure 2 shows the long-term behaviour of (4.1) for various values of β. The initial condition for $L = L_M$ is a single wavenumber perturbation,

$$H(X, 0) = 1 + \delta \cos\left(\frac{2\pi X}{L_M}\right), \tag{4.2}$$

with $\delta = 0.1$. For $\beta = 0$, figure 2(a) shows symmetric self-similar rupture consistent with previous work (Williams & Davis 1982; Zhang & Lister 1999; Witelski & Bernoff 2000). For $\beta = 5$, figure 2(b) still shows rupture, but the rupture is now asymmetric and the rupture time T_R is increased relative to the case $\beta = 0$. For $\beta = 10$, figure 2(c) shows that rupture of the film does not occur over the 50 time units of the calculation. Instead, the disturbance grows to a finite amplitude, and a travelling wave forms. In § 4.2, we provide an asymptotic analysis that confirms the existence of a travelling wave for large β.

https://doi.org/10.1017/S002211201000323X Published online by Cambridge University Press

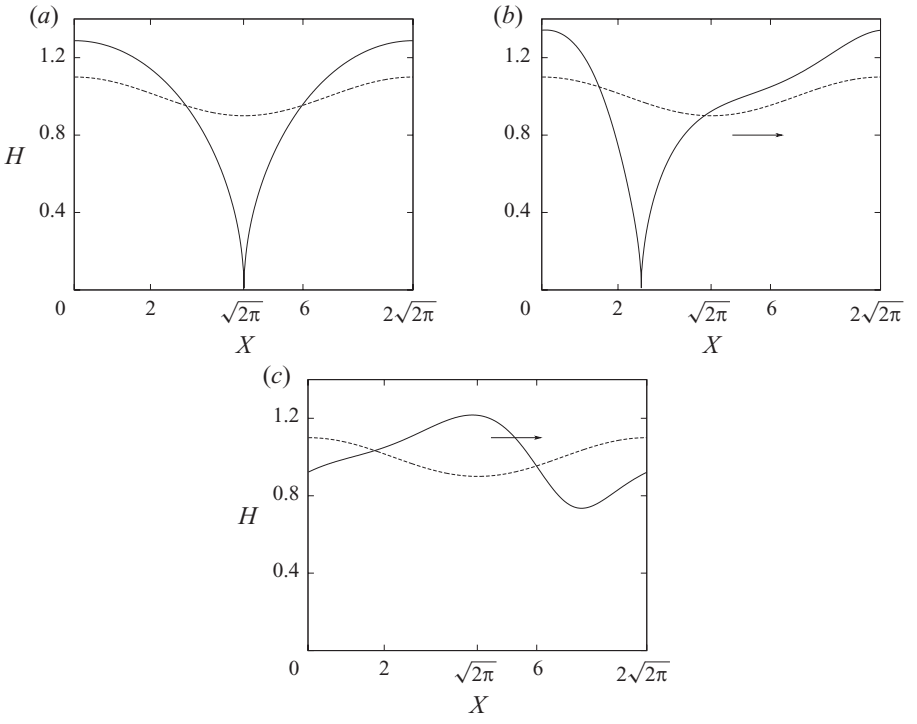


FIGURE 2. Numerical approximations to the film thickness H for various values of β. (a) $\beta = 0$, rupture occurs at $T_R = 4.1$. (b) $\beta = 5$, rupture occurs at $T_R = 5.3$. (c) $\beta = 10$, rupture is suppressed.

Figure 3 shows T_R^{-2} as a function of β. The quantity T_R^{-2} behaves linearly near the critical β, so we extrapolate to predict $\beta_c \approx 9.7$, where β_c divides the behaviour of (4.1) into rupturing and non-rupturing films. It is important to note that whereas these rupture times are specific to a perturbation of $\delta = 0.1$, the value of β_c is applicable to all sufficiently small perturbations. For $\delta \leqslant 0.23$, we find $\beta = \beta_c$ is sufficient for the initial condition to be in the basin of attraction of the travelling wave.

4.2. *Intermolecular-capillary wave instability*

Consistent with the numerical behaviour of (4.1) with $\beta > \beta_c$ and periodic boundary conditions on $[0, L_M]$, we look for a nonlinear travelling-wave solution with wave speed c by introducing a travelling reference frame

$$\eta = X - cT. \tag{4.3}$$

Combining (4.1) and (4.3), we obtain

$$\beta H H_\eta + \left(\frac{H_\eta}{H} + H^3 H_{\eta\eta\eta} \right)_\eta - c H_\eta = 0, \tag{4.4}$$

an ordinary differential equation for $H(\eta)$, where c is determined as an eigenvalue of the nonlinear system. We solve this equation by using asymptotic expansions of the film thickness and wave speed in the limit of $\beta \to \infty$ as follows:

$$H = 1 + \beta^{-1} H_1 + \beta^{-2} H_2 + O(\beta^{-3}), \quad c = \beta c_0 + c_1 + \beta^{-1} c_2 + O(\beta^{-2}). \tag{4.5}$$

https://doi.org/10.1017/S002211201000323X Published online by Cambridge University Press

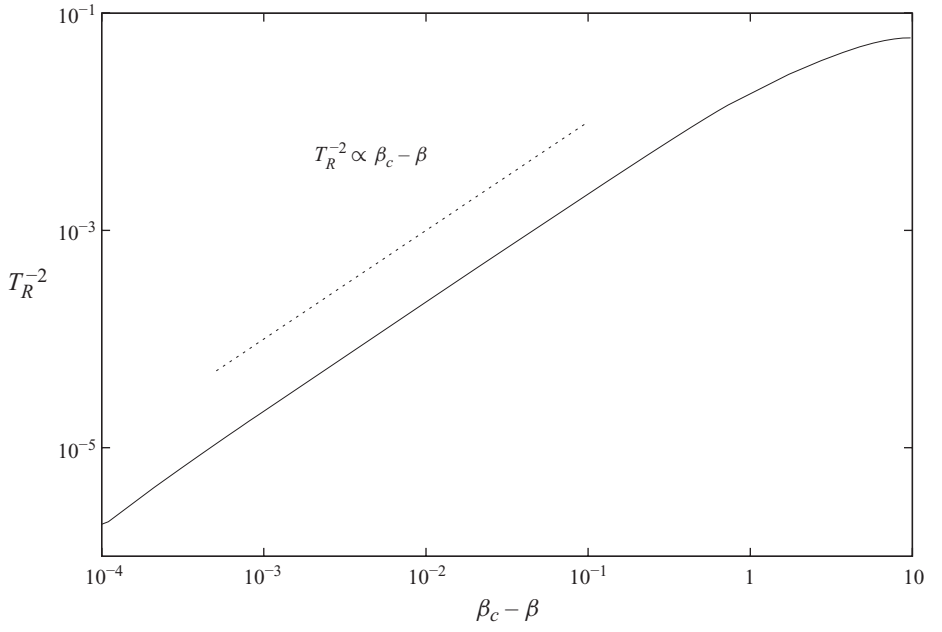


FIGURE 3. Rupture time T_R as a function of the effective shear β. The critical shear for suppressing rupture is $\beta_c \approx 9.7$.

At leading order,

$$(1 - c_0)H_{1\eta} = 0, \tag{4.6}$$

which is satisfied by $c_0 = 1$. At $O(\beta^{-1})$,

$$H_1 H_{1\eta} + H_{1\eta\eta} + H_{1\eta\eta\eta\eta} - c_1 H_{1\eta} = 0. \tag{4.7}$$

This is a nonlinear ordinary differential equation for H_1 with eigenvalue c_1 and must be solved numerically. Doing so yields $c_1 = 0$ and wave shape $H_1(\eta)$. To refine c, we look to the $O(\beta^{-2})$ equation. This may be immediately integrated in η to obtain

$$H_1 H_2 + H_{2\eta} + H_{2\eta\eta\eta} = -c_2 H_1 + H_1 H_{1\eta} - 3H_1 H_{1\eta\eta\eta}. \tag{4.8}$$

Instead of solving this equation, we utilize the Fredholm alternative by considering the adjoint of the homogeneous version of (4.8),

$$H_1 \tilde{H}_2 - \tilde{H}_{2\eta} - \tilde{H}_{2\eta\eta\eta} = 0. \tag{4.9}$$

We choose c_2 so that the right-hand side of (4.8) is orthogonal to the non-trivial solution of (4.9). Doing so gives $c_2 \approx -3.996$, and so

$$c \sim \beta - 3.996\beta^{-1}, \quad \text{as } \beta \to \infty. \tag{4.10}$$

Figure 4 shows the effect of varying β on the film. Figure 4(a) shows the film profiles flattening out as β is varied from 10 to 20. In figure 4(b), we replot the profiles from figure 4(a) to show the deviation from the first asymptotic correction $H_1(\eta)$. Agreement is reasonable for $\beta = 10$ and good for $\beta = 15$. Figure 4(c) shows the wave speed as a function of β as measured numerically compared to the asymptotic wave speed (4.10). The asymptotic analysis thus predicts a non-rupture instability, specifically a permanent travelling wave, for $\beta > \beta_c$. Furthermore, it gives a prediction for both the wave speed and shape of the travelling wave consistent with numerical

https://doi.org/10.1017/S002211201000323X Published online by Cambridge University Press

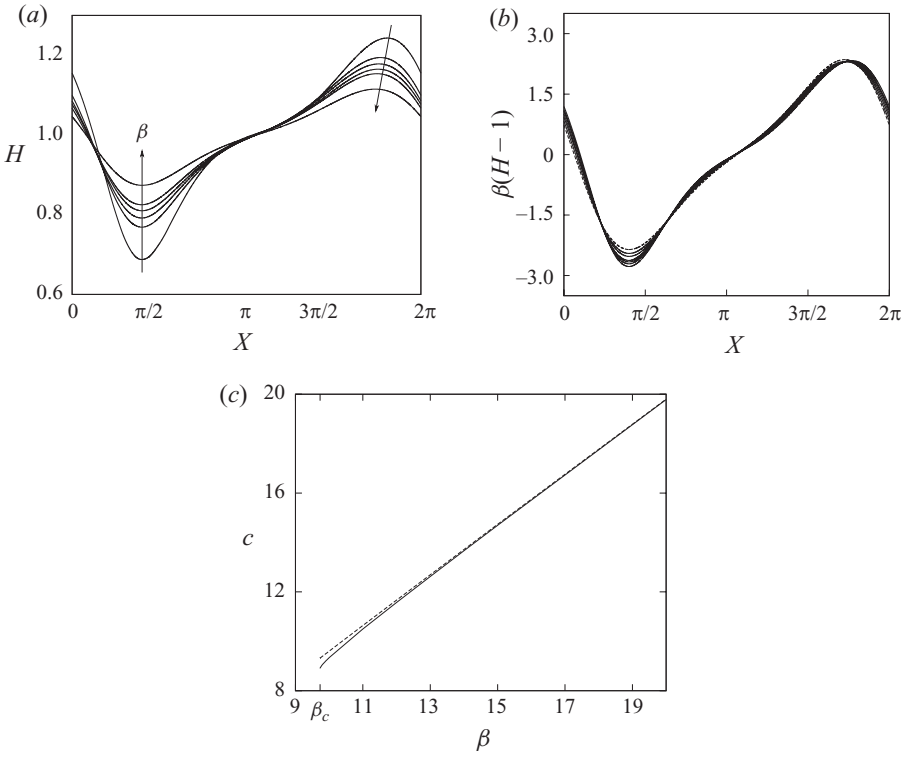


FIGURE 4. Comparison of simulations of (4.1) (solid lines) versus the two-term asymptotic predictions (dashed lines). (*a*) The wave shape for various $10 \leqslant \beta \leqslant 20$. (*b*) The data from (*a*) replotted to extract the deviation from $H = 1$ predicted by the asymptotics: $\beta(1 - H)$ versus X. (*c*) The dependence of the wave speed c on β.

simulations. As expected, the wave speed is proportional to the shear rate β, and therefore, the surface speed. Only the amplitude of the wave depends on β as $\beta \to \infty$. This suggests a simple control over the thinnest point in the film: increasing the shear magnitude decreases the amplitude of H proportionally and makes $H \to 1$ as $\beta \to \infty$.

4.3. *Behaviour for* $k \neq k_M$

We have shown that an applied shear of sufficient magnitude will suppress rupture of a film subjected to van der Waals forces, and lead to a travelling-wave instability. However, the critical shear $\beta_c \approx 9.7$ applies only to disturbances with $k = k_M$. The same analysis may be carried out again for other wavenumbers. Figure 5 shows the numerically determined value of β_c as a function of k. We consider rupture to be suppressed if it does not take place by 50 time units. For larger domains, we allow for longer times, up to $T = 90$. The error bars show the difference in shear magnitude between the largest shear we found that did not suppress rupture and the smallest shear that did suppress rupture.

For $0.5 < k \leqslant 1$, the single cosine-wave perturbation is sufficient for testing stability, as any higher wavenumber that is periodic on this domain will be stable, and therefore, rapidly damped. However, for $k \leqslant 0.5$, more than one unstable mode will fit on the periodic domain. In these cases, we tested both single cosine waves as well as waves

https://doi.org/10.1017/S002211201000323X Published online by Cambridge University Press

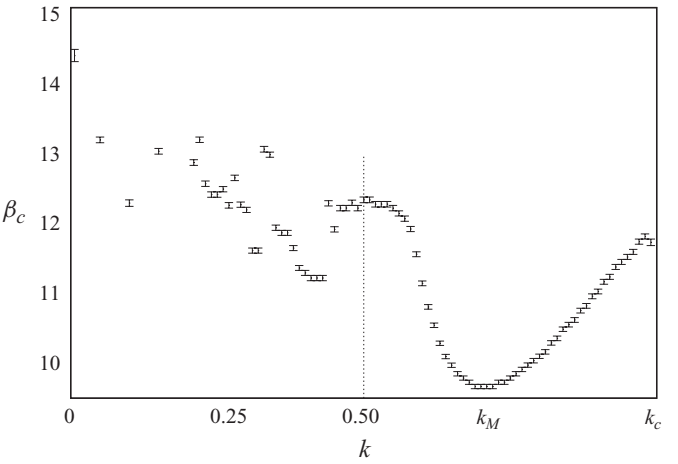


FIGURE 5. The critical shear β_c required to suppress rupture as a function of the largest wavenumber allowed in the periodic domain. Below the curve, the film will rupture. Above it, there is a permanent surface wave.

of the form

$$H(X,0) = 1 + \delta \sum_{n=1}^{N} \left(A_n \cos\left(\frac{2\pi n}{L} X\right) + B_n \sin\left(\frac{2\pi n}{L} X\right)\right), \tag{4.11}$$

where A_n and B_n are randomly chosen uniformly from $[-1, 1]$, N corresponds to the highest frequency unstable mode on $[0, L]$, and δ is chosen such that initial minimum film thickness $H_m = 0.9$. The results for β_c are found to be consistent for various initial conditions. The shear required for suppressing rupture at k_M is actually a minimum; more shear is required to suppress rupture of disturbances at all other unstable wavelengths. For very large domains ($k = 6.3 \times 10^{-2}$), the required shear was not significantly higher than for small domains; a shear of $\beta \approx 15$ would suppress rupture for all values of k we considered. The smallest value of k was chosen to give reasonably long domains, and correspond to physical domains of 1–100 cm, depending on the height scale; see § 6 for more details.

This curve exhibits smooth behaviour for $0.5 \leqslant k \leqslant 1$, but becomes irregular for $k < 0.5$. This change in behaviour can be understood by considering (4.7) without the travelling-wave assumption. Rescaling by

$$X = k^{-1}x, \quad T = k^{-2}t, \quad H_1 = ku \tag{4.12}$$

we obtain

$$u_t + uu_x + u_{xx} + k^2 u_{xxxx} = 0, \tag{4.13}$$

which is the KS equation on $0 \leqslant x < 2\pi$. Note that β only enters this equation through H_1; it simply scales the amplitude. Attracting manifolds for this equation are described by Smyrlis & Papageorgiou (1991) as a function of the bifurcation parameter k^2. They predict a 2π-periodic solution for $0.5 \leqslant k \leqslant 1$, but for $k < 0.5$ predict windows of periodic solutions with periods π, $2\pi/3$ and $\pi/2$, as well as windows of apparent chaotic oscillations. The complex behaviour of the small amplitude equation (4.13) causes the irregular dependence of β_c on k in the fully nonlinear equation (2.6). However, we find similar values of β will suppress rupture in both the period

https://doi.org/10.1017/S002211201000323X Published online by Cambridge University Press

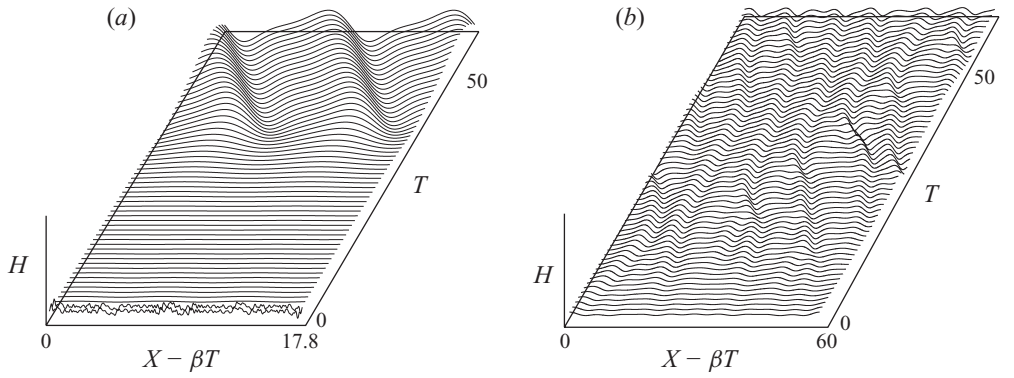


FIGURE 6. (*a*) Period doubling of the travelling wave in the two-dimensional evolution equation for $L = 2L_M$ and $\beta = 15$. (*b*) Non-periodic behaviour for $L = 6.75L_M$ and $\beta = 15$.

multiplying and chaotic oscillation cases of k for sample points chosen in these windows.

Figure 6 shows examples of (*a*) period doubling for $k = k_M/2$ and (*b*) apparent chaotic behaviour for $k = 0.105$ in the numerical solution of (2.6). The domain size to observe these effects agrees with the windows predicted by Smyrlis & Papageorgiou (1991).

5. Suppression of rupture in three dimensions

The analysis of the two-dimensional equation suggests that rupture of thin films can be suppressed when the shear is applied in the direction of disturbance. However, if the domain is larger than L_c in the Y-direction, we must consider the effect of shear on cross-stream perturbations.

To determine the effect of shear on cross-stream perturbations in the X-direction, we examine the initial condition

$$H(X, Y, 0) = 1 + \delta \cos\left(\frac{2\pi X}{L_M}\right), \tag{5.1}$$

on a doubly periodic domain $[0, L_M] \times [0, L_M]$ and evolve with a constant shear in the Y-direction, $\boldsymbol{e} = (0, 1)$. With this initial condition, all Y derivatives vanish, and (2.6) reduces to

$$H_T + (H^3 H_{XXX} + H^{-1} H_X)_X = 0. \tag{5.2}$$

This equation is identical to the unsheared two-dimensional problem, and the evolution will result in rupture in the X-direction while preserving uniformity in the Y-direction. In this case, line rupture will occur in the direction orthogonal to the shear. For the same shear with a more general disturbance,

$$H(X, Y, 0) = 1 + \delta \cos\left(\frac{2\pi X}{L_M}\right) + \delta \cos\left(\frac{2\pi Y}{L_M}\right), \tag{5.3}$$

numerical simulations show the disturbance will develop into a spatially extended travelling wave in the Y-direction whose cross-section is similar to the two-dimensional wave. The disturbance will grow to rupture in the X-direction, resulting in point rupture at the initial minimum in the X-direction, and the minimum of the travelling

https://doi.org/10.1017/S002211201000323X Published online by Cambridge University Press

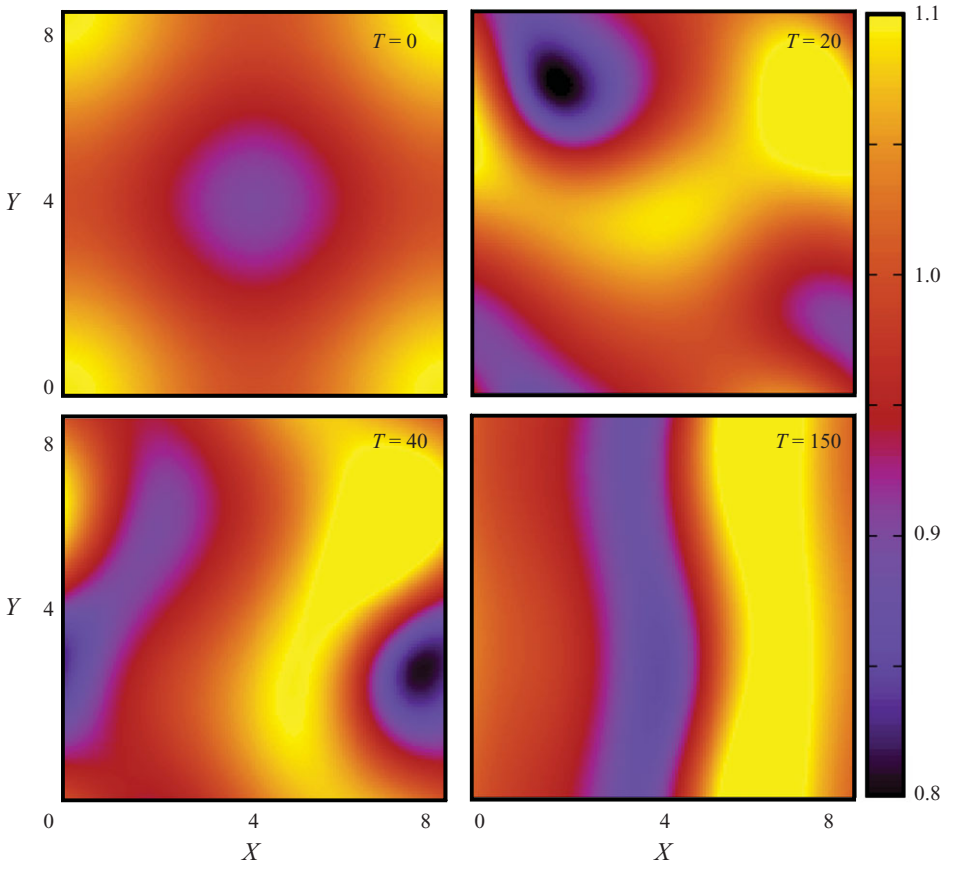


FIGURE 7. The film height $H(X, Y, T)$ for $\beta = 20$ and $\omega = 1$ at different times.

wave in the Y-direction at the time of rupture. Thus a unidirectional shear is incapable of suppressing rupture in the three-dimensional geometry.

We seek a shear protocol that can suppress van der Waals rupture in three-dimensional thin films absolutely. A similar problem was addressed in Schulze & Davis (1995), where a rotating shear was used to suppress a Mullins–Sekerka instability in directional solidification. Similarly, we study the effects of a rotating shear on disturbances

$$H(X, Y, 0) = H_0 + \delta \cos\left(\frac{2\pi X}{L_M}\right) + \delta \cos\left(\frac{2\pi Y}{L_M}\right). \tag{5.4}$$

We again choose $H_0 = 1$, and typically we choose $\delta = 0.05$ so that the initial film minimum is $H_m = 0.9$, the same as in the two-dimensional case. We incorporate the rotation of the shear into the problem by letting the shear direction $\boldsymbol{e}$ vary in T as

$$\boldsymbol{e}(T) = \big(\cos \omega T, \sin \omega T\big). \tag{5.5}$$

A shear protocol consists of the magnitude β and the rotation rate ω.

Figure 7 shows the evolution from the initial condition (5.4) with $\delta = 0.05$ according to (2.6) with shear protocol $(\omega, \beta) = (1, 20)$. At early times ($t = 20$) the minimum grows towards rupture, but by $T = 40$, H features in the Y-direction have become stretched. By $T = 150$, there is only a small variation in the Y-direction and the

https://doi.org/10.1017/S002211201000323X Published online by Cambridge University Press

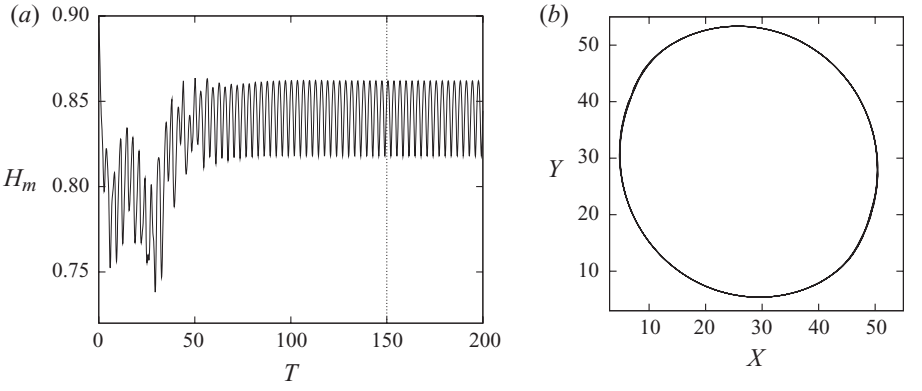


FIGURE 8. (*a*) The minimum film height over the domain as a function of time for a shear of $(\beta, \omega) = (20, 1)$. (*b*) The (X, Y) location of the minimum film height for $150 \leqslant T \leqslant 200$.

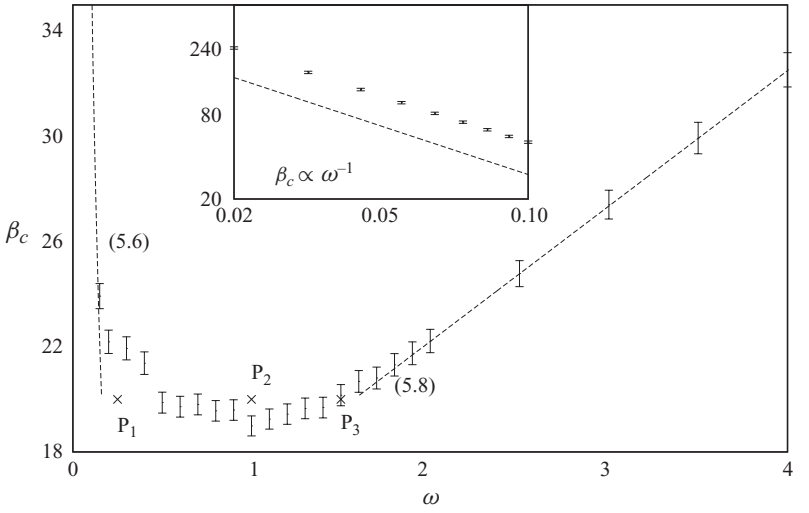


FIGURE 9. The stability curve for three-dimensional films in the $\omega\beta$-plane. Points above the curve are shear protocols that prevent rupture. Dotted lines show asymptotic predictions (5.6) and (5.8). The inset shows $\beta_c(\omega)$ for small ω plotted on a logarithmic scale. The state of the film at rupture (or at $T = 10$ for the stable film) for points P_1, P_2 and P_3 is shown in figure 10.

subsequent dynamics settles onto waves like the one shown for $T = 150$ that translate left and right, tracking the change in direction of the rotating shear. This structure is analogous to the two-dimensional intermolecular-capillary wave. Figure 8(*a*) shows the minimum height H_m as a function of time for the same simulation. For $T \lesssim 60$, H_m appears to be quasi-periodic, but as soon as the initial disturbance in the Y-direction is lost, H_m becomes periodic with its location tracking the circular shear (see figure 8*b*). For larger shears, we sometimes observe quasi-periodic behaviour in both the height and location of the minimum for very long times. This may be related to the two frequencies in the problem: the imposed frequency ω and the travelling-wave 'frequency' c/L_M arising from the periodic boundary conditions.

Examining the shear protocol, we find regions in the $\omega\beta$-plane where rupture is suppressed. Figure 9 shows the suppression boundary calculated by observing when a given shear protocol (ω, β) leads to rupture. The curve represents a lower bound on

https://doi.org/10.1017/S002211201000323X Published online by Cambridge University Press

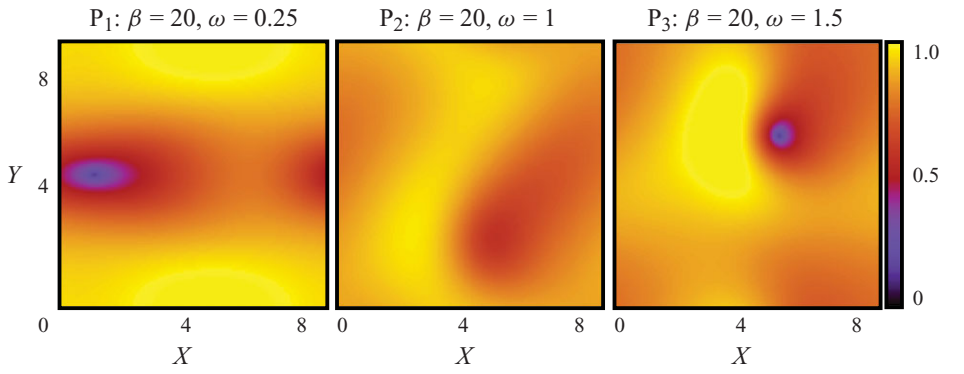


FIGURE 10. The film height at $T = 10$ or at rupture. Shear protocols are as listed. Rupture has been suppressed in the P_2 film. Labels P_1, P_2 and P_3 correspond to points on figure 9.

stability; for each ω, the plotted β_c is the largest β for which we observed rupture. For points P_1, P_2 and P_3, all at $\beta = 20$ but with different ω, the dynamics of the film with the corresponding (ω, β) is shown in figure 10. Near point P_1, the film is susceptible to line rupture, as ω is small enough that the shear is essentially unidirectional for long enough that rupture occurs in the transverse direction. Point rupture is observed here only because the initial condition (5.4) is not symmetric in X. Near point P_2, the film does not rupture, but instead exhibits the three-dimensional wave instability shown in figure 7. Near point P_3, ω is large enough that the shear does not spend enough time in a given direction to suppress perturbation growth, and the film is susceptible to point rupture. The shear moves disturbances in the film in circles, but the amplitude still grows until the film dewets. The shear protocol that requires the lowest magnitude for stability (ω_*, β_*) occurs at approximately (1, 20). It is interesting that the optimal ω_* is neither large nor small compared to the time scale (2.5). The minimum shear strength β_* is about twice the value required to suppress rupture in a two-dimensional film at $L = L_M$.

In the limit of both small and large rotation frequency, the dependence of the stability curve on ω may be understood. For $\omega \ll 1$, we have that $\beta \boldsymbol{e}_1 = \beta \cos(\omega T) = \beta + O((\omega T)^2)$ and $\beta \boldsymbol{e}_2 = \beta \sin(\omega T) = \beta\omega t + O((\omega T)^3)$. Provided $\beta > \beta_c$, rupture will be suppressed in the X-direction. In the Y-direction, the shear magnitude now grows in time proportional to ω, so we must have

$$\beta_c \propto \omega^{-1}, \quad \text{as} \quad \omega \to 0 \tag{5.6}$$

to suppress rupture in the Y-direction. This trend is shown in the inset of figure 9. In the two-dimensional equation (4.1), a shear $\beta\omega T$ results in a stability relation $\beta_c \omega \approx 2.2$. This is qualitatively similar to the observed $\beta_c \approx 4.8/\omega + 2.6$ fit for three dimensions.

When $\omega \gg 1$, we can rescale time in (2.6) by $1/\omega$ to see

$$H_T + \frac{\beta}{\omega}(\cos T, \sin T)\cdot(H\nabla H) + \frac{1}{\omega}\nabla\cdot(H^3\nabla\nabla^2 H + \nabla H H^{-1}) = 0. \tag{5.7}$$

If the dynamics are to be controlled by shear, we expect the coefficient multiplying the shear term to be $O(1)$ for any ω, so

$$\beta_c \propto \omega, \quad \text{as} \quad \omega \to \infty. \tag{5.8}$$

https://doi.org/10.1017/S002211201000323X Published online by Cambridge University Press

Fitting the computed stability boundary yields $\beta_c \approx 5\omega + 13$. Solving the two-dimensional equation (4.1) on $0 \leqslant X < L_M$ subject to $\beta = \cos(\omega T)$ also yields $\beta_c \propto \omega$, though with a different constant.

In two dimensions, figure 5 shows that the smallest value of β_c is obtained for k_M. In domains of other sizes, for suppression the shear must be increased by as much as 35 %. In three dimensions, calculations for a domain of $k = 0.9$ show that at $\omega = 1$, $\beta_c \approx 25$, an increase in the required shear for suppression by about 25 %. This is comparable to the 20 % increase in β_c observed in two dimensions when changing from $k = k_M$ to $k = 0.9$ (see figure 5). It is reasonable to expect that the stability curve shown in figure 9 is an underestimate of the shear strength required to suppress rupture in films on more general domains. More detailed calculations are not warranted because the protocol is only illustrative of shear suppression (see § 6).

6. Discussion

We have shown that a constant applied shear stress of sufficient magnitude, $\beta_c \approx 9.7$, can suppress rupture of a bounded film in two dimensions for $L = L_M$ and replaces such a state by a nonlinear travelling intermolecular-capillary wave. In three dimensions, a shear stress of large enough constant magnitude, $\beta_* \approx 20$, rotating at angular speed $\omega_* \approx 0.5$ has a similar effect, again for $L = L_M$. For larger domains, the appearance of smaller wavenumbers increases the value of the critical shear, but this appears to be bounded. Large domains may exhibit chaotic behaviour, but the amplitude of oscillation is fixed.

We can gain some rough understanding of the suppression of rupture by noting that it occurs when β is about an order of magnitude larger that the scale of the van der Waals term. Scaling (4.1) by

$$h = \left(\frac{A}{S}\right)^{1/4} H, \quad \bar{x} = \left(\frac{A}{S}\right)^{1/2}, \quad \bar{t} = \left(\frac{A}{S}\right)^{1/4} T, \tag{6.1}$$

we remove the scaling on H and scale X consistent with k_M from (2.10). We obtain

$$h_{\bar{t}} + \beta h h_{\bar{x}} + \left(\frac{A}{S}\right)(h^3 h_{\bar{x}\bar{x}\bar{x}} + h^{-1} h_{\bar{x}})_{\bar{x}} = 0. \tag{6.2}$$

The shear term will dominate the van der Waals term when $\beta \gg A/S$. Rewriting the expression in dimensional terms gives

$$\tau \gg \left(\frac{A}{2\pi\sigma^{1/3}}\right)^{3/2} h_o^{-4}, \tag{6.3}$$

where $[A/(2\pi\sigma^{1/3})]^{3/2} \approx 6.2 \times 10^{-21}$ dyn cm^2. Changing the thickness of the basic state by a factor of 10 changes the required shear by a factor of 10 000.

We now determine the numerically predicted magnitude of shear required to prevent rupture in a prototype experiment. Table 1 shows the magnitude of the shear τ required to stabilize a layer of thickness h_o. Here, we assume that the film is thick enough that bulk properties are present. We use $A^* = 10^{-13}$ erg, a typical value used by Vrij (1966). For the fluid properties, we use $\sigma = 10^2$ dyn cm^{-1}, $\rho = 1$ g cm^{-1} and $\mu = 1$ cP, similar to those of water. For these parameters, $S \approx 10^{-10}$. The length scale is linked to h_o through the aspect ratio ε, which we take to be 10^{-3}. The shear is computed from (2.7) using the approximate magnitude of β_c at $k = k_M$ for the three values of h_o in the table. For $h_o = 10^{-5}$ cm, we use the data from figure 3

https://doi.org/10.1017/S002211201000323X Published online by Cambridge University Press

h_o (cm)	β_c	τ (dyn cm^{-2})	A/S	U_s (cm s^{-1})	length scale (cm)	time scale (s)
10^{-4}	10^{-1}	10^{-6}	10^{-2}	10^{-8}	10^{-1}	10^{3}
10^{-5}	10	10^{-2}	10^{0}	10^{-5}	10^{-2}	10^{0}
10^{-6}	10^{3}	10^{2}	10^{2}	10^{-2}	10^{-3}	10^{-2}

TABLE 1. The magnitude of the shear needed to stabilize a layer of thickness h_o for material properties similar to water. These order of magnitude numbers apply to both the two- and three-dimensional cases at any domain size.

for β_c. For $h_o \neq 10^{-5}$ cm, we find β_c numerically using the same technique. The shear strength can be compared to the relative scale of surface tension and van der Waals terms, A/S. The capillary-velocity scale $\sigma/\mu = 10^4$ cm s^{-1} is quite large compared to the shear velocity scale $U_s = \tau h_o/\mu$ for all values of h_o and β_c. The largest calculation performed in two dimensions ($L = 1000$) corresponds to a domain of 1 cm at $h_o = 10^{-5}$, a physically reasonable dimension for many applications. The corresponding time scale for $h_o = 10^{-5}$ is about 1 s, so a shear of non-dimensional angular frequency $\omega = 1$ has a dimensional circular frequency of 1 rad s^{-1}. Table 1 thus shows that shear stabilization requires only a modest impositions of shear provided the film is not too thin. Moreover, the scaling prediction of (6.3) is borne out in the table: β_c is an order of magnitude larger than A/S in all cases, and $\tau \propto h_o^{-4}$.

The stabilization in three dimensions utilizes a constant shear rotating at a constant angular speed. We make no claim that this is an optimal protocol, at least in the sense that it would provide suppression for the smallest shear magnitude. It is merely an example of a forcing that totally suppresses rupture. Other related shear protocols could stabilize a film against rupture. The rotating shear protocol could be achieved in the lab by rotating the substrate so that a constant unidirectional shear becomes a rotating shear in the frame of the film. Surface stirring shears, with a single point of rotation that experiences no shear will likely fail, as near the centre of rotation there will always be some region where the shear strength is below critical. Another possibility is to approximate rotation with a discrete periodic shear, where there are only a handful of shear directions that are sheared in succession. This avoids a rotating substrate, but would require several sources of shear. More work will be needed to understand which shear protocols are desirable.

Physically, the mechanism by which a shear stabilizes a film can be seen from the dependence of β on the system parameters (2.7). The nonlinear nature of the shear term is such that higher regions of the film move faster. This causes the ridges around a developing hole to steepen, exciting capillary forces to stabilize the film. Such structures are visible in figure 2. The dependence of β on $\sigma^{-1/2}$ seen in (2.7) shows that films with stronger surface tensions would require less shear to be stabilized. While it appears paradoxical that β also depends on $(A^*)^{-1/2}$, without van der Waals forces the rescaling (2.5) can no longer apply. Mathematically, the transition from rupturing states to bounded states could be better understood in the context of weakly nonlinear analysis.

It is natural to wonder, if such small magnitudes of shear are needed to suppress rupture, why falling films are still subject to it. While the dynamics of small-amplitude disturbances we observe are similar to those for falling films, the Benney equation (Benney 1966) for thick films and thin films on inclined substrates, the use of gravity or any body force to generate shear will require at least an $O(h_o^{-1})$ extra factor of

https://doi.org/10.1017/S002211201000323X Published online by Cambridge University Press

shear for stability. Particularly, in the evolution equation for the height of a thin film on a vertical substrate (1.3), the magnitude of the hyperbolic term is controlled by

$$m_b = 3\rho g \left(\frac{2\pi}{\sigma^3 A^*}\right)^{1/4} \left(\frac{h_o^{5/2}}{\varepsilon}\right), \tag{6.4}$$

which can be compared to (2.7). The role of τ is played by ρg, while a factor of $h_0^{1/2}/\varepsilon$ is missing. For the parameter scales used in table 1 with $h_o = 10^{-5}$ cm and $\rho = 1\,\mathrm{g\,cm^{-3}}$, the falling film m_b would be equivalent to a shear of $\tau = 10^{-7}$ dyn cm^2. This is five orders of magnitude too small for stabilization. If a falling film were to experience the equivalent shear that stabilizes such a film (albeit with a different hyperbolic term), $\rho g = 10^8\,\mathrm{g\,cm^{-2}\ s^{-2}}$. Terrestrial gravity is not strong enough to provide this magnitude of shear. It may be feasible for other body forces, such as electric forces, to be large enough for rupture suppression.

We are grateful to P. S. Stewart for his insight into the convective instability and A. M. Anderson for several enlightening discussions. M.J.D. and S.H.D. acknowledge support from National Science Foundation Grant CMMI-0826703. M.B.G. acknowledges support from National Science Foundation RTG Grant DMS-0636574.

REFERENCES

Anderson, A. M., Brush, L. N. & Davis, S. H. 2010 Foam mechanics: spontaneous rupture of thinning liquid films with Plateau borders. *J. Fluid Mech.* doi:10.1017/s0022112010001527.

Benney, D. J. 1966 Long waves in liquid film. *J. Math. Phys.* **45**, 150–155.

Bielarz, C. & Kalliadasis, S. 2003 Time-dependent free-surface thin film flows over topography. *Phys. Fluids* **15** (9), 2512–2524.

Chang, H.-C. 1994 Wave evolution on a falling film. *Annu. Rev. Fluid. Mech.* **26**, 103–136.

Chang, H.-C., Demekhin, E. A., Kalaidin, E. & Ye, Y. 1996 Coarsening dynamics of falling-film solitary waves. *Phys. Rev.* E **54** (2), 1467–1477.

Coons, J. E., Halley, P. J., McGlashan, S. A. & Tran-Cong, T. 2003 A review of drainage and spontaneous rupture in free standing thin films with tangentially immobile interfaces. *Adv. Colloid Interface Sci.* **105** (1–3), 3–62.

Erneux, T. & Davis, S. H. 1993 Nonlinear rupture of free films. *Phys. Fluids* A **5** (5), 1117–1122.

Gumerman, R. J. & Homsy, G. M. 1975 The stability of radially bounded thin films. *Chem. Engng Commun.* **2**, 27–36.

Holly, F. J. 1973 Formation and rupture of the tear film. *Exp. Eye Res.* **15** (5), 515–525.

Ida, M. P. & Miksis, M. J. 1998 The dynamics of thin films. Part I. General theory. *SIAM J. Appl. Maths* **58** (2), 456–473.

Jacobs, K., Herminghaus, S. & Mecke, K. R. 1998 Thin liquid polymer films rupture via defects. *Langmuir* **14** (4), 965–969.

Kalpathy, S. K., Francis, L. F. & Kumar, S. 2010 Shear-induced suppression of rupture in two-layer thin liquid films. *J. Colloid Interface Sci.* **348** (1), 271–279.

King-Smith, E., Fink, B., Hill, R., Koelling, K. & Tiffany, J. 2004 The thickness of the tear film. *Curr. Eye Res.* **29** (4–5), 357–368.

Lenz, R. D. & Kumar, S. 2007 Competitive displacement of thin liquid films on chemically patterned substrates. *J. Fluid Mech.* **571**, 33–57.

Oron, A., Davis, S. H. & Bankoff, S. G. 1997 Long-scale evolution of thin liquid films. *Rev. Mod. Phys.* **69**, 931–980.

Reiter, G. 1992 Dewetting of thin polymer films. *Phys. Rev. Lett.* **68** (1), 75–78.

Ruckenstein, E. & Jain, R. K. 1974 Spontaneous rupture of thin liquid films. *J. Chem. Soc. Faraday Trans. 2* **70**, 132.

https://doi.org/10.1017/S002211201000323X Published online by Cambridge University Press

Schenk, O., Bollhoefer, M. & Roemer, R. 2008 On large-scale diagonalization techniques for the Anderson model of localization. *SIAM Rev.* **50**, 91–112.

Schenk, O., Waecher, A. & Hagermann, M. 2007 Matching-based preprocessing algorithms to the solution of saddle-point problems in large-scale nonconvex interior-point optimization. *J. Comput. Optim. Appl.* **36** (2–3), 321–341.

Schulze, T. P. & Davis, S. H. 1995 Shear stabilization of morphological instability during directional solidification. *J. Cryst. Growth* **149**, 253–265.

Sharma, A. & Ruckenstein, E. 1986 Finite-amplitude instability of thin free and wetting films: predition of lifetimes. *Langmuir* **2**, 480–494.

Sheludko, A. 1967 Thin liquid films. *Adv. Colloid Interface Sci.* **1** (4), 391.

Smyrlis, Y. S. & Papageorgiou, D. T. 1991 Chaos for infinite dimensional dynamical systems: the Kuramoto–Sivashinsky equation, a case study. *Proc. Natl Acad. Sci. USA* **88**, 11129–11132.

Teletzke, G. F., Davis, H. T. & Scriven, L. E. 1988 Wetting hydrodynamics. *Rev. Phys. Appl.* **23**, 989–1007.

Thiele, U. & Knobloch, E. 2004 Thin liquid films on a slightly inclined heated plate. *Physica* D **190**, 213–248.

Thiele, U., Neuffer, K., Bestehorn, M., Pomeau, Y. & Velarde, M. G. 2002 Sliding drops on an inclined plane. *Colloids Surf.* A **206**, 87–104.

Tseluiko, D. & Papageorgiou, D. T. 2006*a* A global attracting set for nonlocal Kuramoto–Sivashinsky equations arising in interfacial electrohydrodynamics. *Eur. J. Appl. Maths* **17**, 677–703.

Tseluiko, D. & Papageorgiou, D. T. 2006*b* Wave evolution on electrified falling films. *J. Fluid Mech.* **556**, 361–386.

Vaynblat, D., Lister, J. R. & Witelski, T. P. 2001 Rupture of thin viscous films by van der Waals forces: evolution and self-similarity. *Phys. Fluids* **13**, 1130–1140.

Vignes-Adler, M. 2002 *Physico-Chemical Aspects of Forced Wetting*, chap. 4, pp. 103–157. Springer.

Vrij, A. 1966 Possible mechanism for the spontaneous rupture of thin, free liquid films. *Discuss. Faraday Soc.* **43**, 23.

Williams, M. B. & Davis, S. H. 1982 Nonlinear theory of film rupture. *J. Colloid Interface Sci.* **90** (1), 220–228.

Witelski, T. P. & Bernoff, A. J. 2000 Dynamics of three-dimensional thin film rupture. *Physica* D **147** (1–2), 155–176.

Zhang, W. W. & Lister, J. R. 1999 Similarity solutions for van der Waals rupture of a thin film on a solid substrate. *Phys. Fluids* **11** (9), 2454–2462.

https://doi.org/10.1017/S002211201000323X Published online by Cambridge University Press